J|A|C|S
ARTICLES
Published on Web 07/12/2005

Mycosamine Orientation of Amphotericin B Controlling Interaction with Ergosterol: Sterol-Dependent Activity of Conformation-Restricted Derivatives with an Amino-Carbonyl Bridge

Nobuaki Matsumori, Yuri Sawada, and Michio Murata*

Contribution from the Department of Chemistry, Graduate School of Science, Osaka University, Toyonaka, Osaka 560-0043, Japan

Received March 12, 2005; E-mail: murata@ch.wani.osaka-u.ac.jp

Abstract: Amphotericin B (AmB **1**) is known to assemble together and form an ion channel across biomembranes. The antibiotic consists of mycosamine and macrolactone moieties, whose relative geometry is speculated to be determinant for the drug's channel activity and sterol selectivity. To better understand the relationship between the amino-sugar orientation and drug's activity, we prepared conformation-restricted derivatives **2**−**4**, in which the amino and carboxyl groups were bridged together with various lengths of alkyl chains. K^+ influx assays across the lipid-bilayer membrane revealed that ergosterol selectivity was markedly different among derivatives; short-bridged derivative **2** almost lost the selectivity, while **3** showed higher ergosterol preference than AmB itself. Monte Carlo conformational analysis of **2**−**4** based on NOE-derived distances indicated that the amino-sugar moiety of **2** comes close to C41 because of the short bridge, whereas those of **3** and **4** are pointing outward. The mutual orientation of the amino-sugar moiety and macrolide ring is so rigid in derivatives **2** and **3** that these conformations should be unchanged upon complex formation in lipid membranes. These results strongly suggest that the large difference in sterol preference between derivatives **2** and **3** is ascribed to the different orientation of amino-sugar moieties. These findings allowed us to propose a simple model accounting for AmB−sterol interactions, in which hydrogen bonding between 2′-OH of AmB and 3β-OH of ergosterol plays an important role.

Introduction

For over 40 years, amphotericin B (AmB, **1**) (Chart 1) has been a standard drug for treatment of deep-seated systemic fungal infections, which are a continuing and growing concern for the management of immunocompromised patients infected by HIV.[1−3] Due to lack of better alternatives coupled with the infrequency of occurrence of opportunistic resistance in fungal strains,[4] the clinical importance of AmB has even been enhanced. It is now widely accepted that AmB in phospholipid membrane associates with sterols to form barrel-stave type pores, where the AmB molecules are arranged in a quasi-parallel orientation, their polyhydroxy side pointing inward to constitute the pore lining and their lipophilic heptaene part directing outward to interact with the membrane interior (Figure 1).[5,6] The presence of such molecular assemblages in cell membrane of fungi increases ion permeability and alters membrane potentials, ultimately leading to the cell death.[6−9] The pharmacological action of AmB is based on its selective toxicity against eukaryotic microbes over mammalians. It has been repeatedly shown that ergosterol-containing fungal membranes are more sensitive to AmB than cholesterol-containing mammalian membranes.[8,10,11] Consequently, the concentration of AmB

Chart 1. Structures of AmB **1**, Ergosterol, and Cholesterol

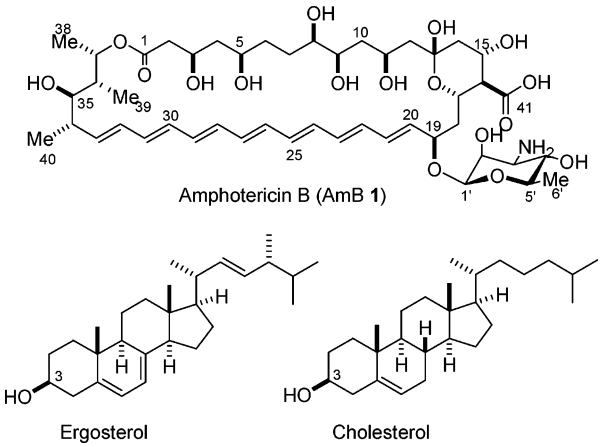

(1) Gallis, H. A.; Drew, R. H.; Pckard, W. W. *Rev. Infect. Dis*. **1990**, *12*, 308−329.
(2) Hartsel, S. C.; Bolard, J. *Trends Pharmacol. Sci.* **1996**, *12*, 445−449.
(3) Ablordeppey, S. Y.; Fan, P. C.; Ablordeppey, J. H.; Mardenborough, L. *Curr. Med. Chem*. **1999**, *6*, 1151−1195.
(4) Vanden-Bossche, H.; Dromer, F.; Improvisi, I.; LozanoChiu, M.; Rex, J. H.; Sanglard, D. *Med. Mycol*. **1998**, *36*, 119−128.
(5) Andreoli, T. E. *Ann. N.Y. Acad. Sci.* **1974**, *235*, 448−468.
(6) De-Kruijff, B.; Demel, R. A. *Biochim. Biophys. Acta* **1974**, *339*, 57−70.
(7) Cohen, B. E. *Biochim. Biophys. Acta* **1986**, *857*, 117−122.
(8) Vertut-Croquin, A.; Bolard, J.; Chabbert, M.; Gary-Bobo, C. *Biochemistry* **1983**, *22*, 2939−2944.
(9) Van-Hoogevest, P.; De-Kruijff, B. *Biochim. Biophys. Acta* **1978**, *511*, 397−407.
(10) Milhaud, J.; Hartman, M. A.; Bolard, J. *Biochimie* **1989**, *71*, 49−56.

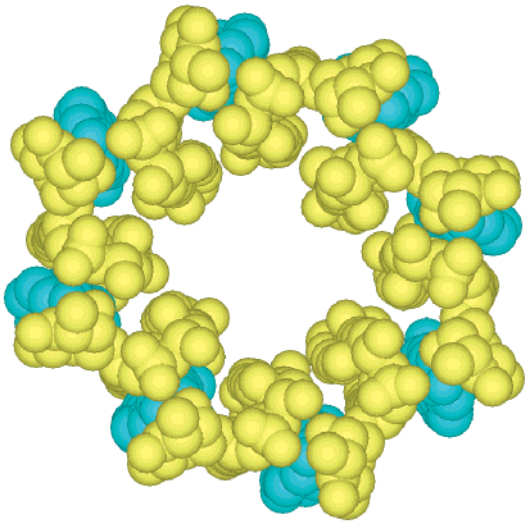

Figure 1. Hypothetical structure of a "barrel-stave" ion channel formed by 8 AmBs and 8 sterols. Yellow and blue molecules represent AmB and sterol, respectively.[5,6]

necessary to elicit the lethal permeability is higher with cholesterol than with ergosterol.

Extensive experimental efforts, ranging from spectroscopic measurements[12] to electrophysiological examinations, have so far been made to comprehensively understand the molecular basis of the trans-membrane pore formed by AmB. However, two conventional methods for structural biology, X-ray crystallography and liquid NMR, are hardly applicable to membrane-bound entities, hence leaving the molecular architecture of the AmB's ion-permeable channel unelucidated. During the past decade, various computational approaches have also been carried out pursuing structural factors involved in the channel formation of AmB and its specificity toward ergosterol.[13] Despite the potentiality of these approaches, further accumulation of experimental data on the AmB complex is essential to improve the accuracy of computer simulations. The overall structure of AmB comprises two rigid fragments, a macrolide ring and a mycosamine sugar moiety, which are linked by a rotatable β-glycosidic bond. Their relative position is thought to partly control AmB−AmB and AmB−sterol interactions, where inter- and intramolecular hydrogen bonds should play a crucial role.[13d,h] Resat et al. hypothesized that the relative orientation of the amino sugar with respect to the macrolide portion influences the selective toxicity of the drug.[13g] In their model, the channel structure was stabilized by sterol molecules, which reside close to AmB by their hydrophobic interactions, subsequently resulting in the higher selectivity of ergosterol over

Chart 2. Structures of Intramolecular Bridged Derivatives **2**−**4** and Open-Bridged **5**

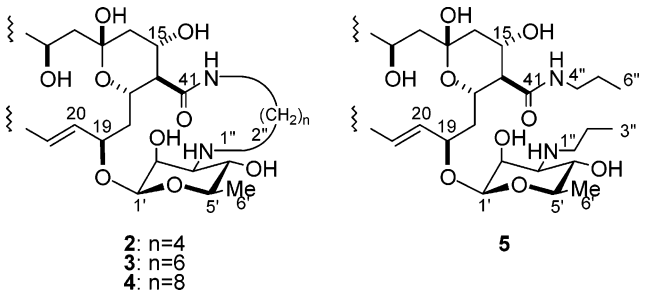

2: n=4
3: n=6
4: n=8

5

cholesterol. So far, however, there has been no experimental evidence accounting for the sterol selectivity in terms of the conformation of AmB.

In this report, to gain insight into the conformation−activity relationship, particularly for the glycosidic bond, we prepared conformationally restricted derivatives of AmB **2**−**4** (Chart 2), where intramolecular carboxyl and amino groups are bridged together with various lengths of alkyl chains. These bridges greatly restrict the rotational freedom around glycoside bonds and may desirably allow for a single conformation. If this is the case, it should be possible to deduce the active conformation of the amino-sugar of AmB upon complexation in the ion channel; the bridges of derivatives **2**−**4** are expected to minimize the conformational difference between a sugar orientation in solution and that in the channel complex. Consequently, **2**−**4** showed markedly variable ergosterol preference in K^+ influx assays, which can be interpreted with respect to the alteration of the amino-sugar position induced by alkyl bridges. On the basis of these results, we discuss the relationship between the ergosterol selectivity and orientation of the amino-sugar moiety.

Results

Preparation of Conformationally Restricted AmB Derivatives. We prepared three conformationally constrained derivatives of AmB (**2**, **3**, and **4**), where carboxyl and amino groups of AmB are intramolecularly linked with C_4, C_6, and C_8 alkyl chain bridges, respectively. These derivatives were expected to adopt different relative orientations between the amino-sugar and macrolide ring. This molecular design is rational in the light of previous reports on the structure−activity relationship; the presence of the amino group is reportedly essential for the antibiotic activity, and the protection of the free carboxyl group by esterification or amidation has little influence on the membrane activity or sterol selectivity, which suggests that the relatively rigid conformation of the macrolide ring is hardly affected by charge on the carboxylic acid.[14] The synthetic route of derivatives **2**−**4** is represented in Scheme 1. Amino alcohols with *n*-butyl, hexyl, and octyl chains were first protected with an Fmoc group, and then converted to aldehydes by SO_3-pyridine or Swern oxidation. The aldehydes were coupled with the amino group of AmB by the reductive amino-alkylation with use of $NaBH_3CN$. Deprotection of the Fmoc group followed by intramolecular amide formation in the presence of PyBOP

(11) Vertut-Qroquin, A.; Bolard, J.; Gary-Bobo, C. M. *Biochem. Biophys. Res. Commun*. **1984**, *125*, 360−366.
(12) Recent examples are: (a) Fujii, G.; Chang, J. E.; Coley, T.; Steere, B. *Biochemistry* **1997**, *36*, 4959−4968. (b) Gago, M.; Koper, R.; Gruszecki, W. I. *Biochim. Biophys. Acta* **2001**, *1511*, 90−98.
(13) Selected publications are: (a) Baginski, M.; Borowski, E. *THEOCHEM* **1997**, *389*, 139−146. (b) Baginski, M.; Bruni, P.; Borowski, E. *THEOCHEM* **1994**, *311*, 285−296. (c) Mazerski, J.; Borowski, E. *Biophys. Chem.* **1996**, *57*, 205−217. (d) Baginski, M.; Gariboldi, P.; Bruni, P.; Borowski, E. *Biophys. Chem.* **1997**, *65*, 91−100. (e) Baginski, M.; Resat, H.; McCammon, J. A. *Mol. Pharmacol.* **1997**, *52*, 560−570. (f) Silberstein, A. *J. Membr. Biol.* **1998**, *162*, 117−126. (g) Resat, H.; Sungur, F. A.; Baginski, M.; Borowski, E.; Aviyente, V. *J. Comput.-Aided Mol. Des.* **2000**, *14*, 689−703. (h) Baginski, M.; Resat, H.; Borowski, E. *Biochim. Biophys. Acta* **2002**, *1567*, 63−78. (i) Mariusz Baran, M.; Mazerski, J. *Biophys. Chem.* **2002**, *95*, 125−133. (j) Langlet, J.; Berges, J.; Caillet, J.; Demaret, J. P. *Biochim. Biophys. Acta* **1994**, *1191*, 79−93. (k) Sternal, K.; Czub, J.; Baginski, M. *J. Mol. Model.* **2004**, *10*, 223−232.
(14) (a) Cheron, M.; Cybulska, B.; Mazerski, J.; Grzybowska, J.; Czerwinski, A.; Borowski, E. *Biochem. Pharmacol.* **1988**, *37*, 827−836. (b) Mazerski, J.; Bolard, J.; Borowski, E. *Biochim. Biophys. Acta* **1995**, *1236*, 170−176. (c) Jarzebski, A.; Falkowski, L.; Borowski, E. *J. Antibiot.* **1982**, *35*, 220−229. (c) Mazerski, J.; Bolard, J.; Borowski, E. *Biochim. Biophys. Acta* **1995**, *1236*, 170−176.

Scheme 1. Preparation of **2**−**5**[a]

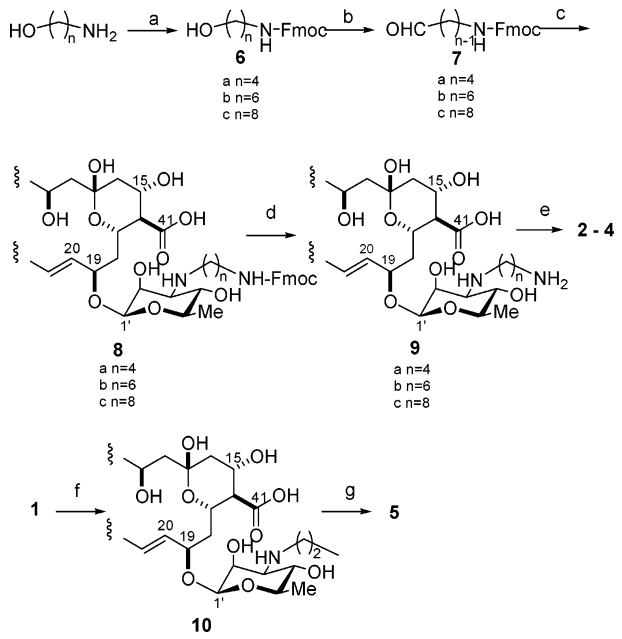

[a] Reagents: (a) Fmoc−OSu, pyridine, MeOH; (b) SO_3−pyridine, triethylamine, DMSO; or $(COCl)_2$, DMSO, triethylamine, CH_2Cl_2; (c) AmB, $NaBH_3CN$, DMF−MeOH; (d) piperidine, DMF−MeOH; (e) PyBOP, HOBt, *N*-ethyldiisopropylamine, DMF; (f) propionaldehyde, $NaBH_3CN$, DMF−MeOH; (g) aminopropane, PyBOP, HOBt, *N*-ethyldiisopropylamine, DMF (for product yield in each step, see Experimental Section).

as a condensation reagent afforded bridged derivatives **2**−**4**. We also attempted to prepare a derivative with a propyl chain bridge, but the objective compound could not be obtained. This indicates the spatial distance between the carboxyl and amino groups is beyond the reach of the maximum length of the aminopropyl chain, ca. 0.5 nm, or the compound might be decomposed, once formed, due to the strain of the short bridge. To evaluate the influence of the alkyl chains substituted at the amino and carboxylic acid groups, we also prepared **5**, an open-bridged congener of **3**. This compound was obtained by the reductive aminoalkylation of AmB's amino group with propanal, followed by the amidation of the carboxyl group with *n*-propylamine (Scheme 1).

K^+ Flux Assay Using Liposomes. We then assessed the K^+ flux activity of these derivatives across lipid bilayer membrane using a method reported by Herve et al.[15,16] In this assay, K^+ concentration was higher outside with trans-membrane pH gradient (pH 5.5 inside and pH 7.5 outside). Once ion channels form, K^+ influx into liposomes induces H^+/K^+ exchange in the presence of proton-transporter FCCP, leading to a rise in inner pH. The increase in inner pH was monitored by chemical shift changes of phosphate anions in ^{31}P NMR; a downfield signal at δ 3.1 stems from phosphate ions entrapped in liposomes where inside pH rose due to the channel formation, while an upfield signal at δ 1.2 is due to phosphate in intact liposomes. Signals of phosphate ions outside the liposomes were quenched by paramagnetic Mn^{2+} ions. Accordingly, channel activity of the drugs can be estimated from the decrease in peak intensity at δ 1.2 or increase at δ 3.1. The spectral features of ^{31}P NMR

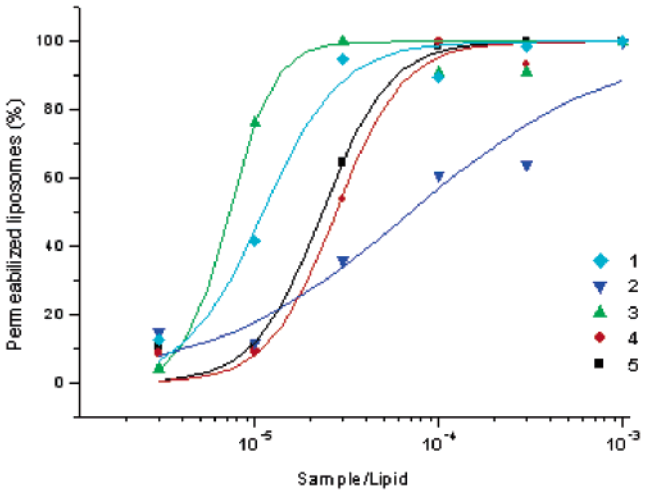

Figure 2. Concentration−effect relationship of K^+ influx activities for AmB (**1**) and its analogues **2**−**5** in ergosterol-containing liposomes. Liposomes were composed of egg-phosphatidylcholine (PC) and ergosterol at the ratio of 9:1, and lipid concentration (eggPC plus ergosterol) in a liposome suspension was 12 mM. The *y* axis denotes the ratio of permeabilized liposomes, which was determined from a decrease in peak area at δ 1.2 in ^{31}P NMR spectra.

Table 1. K^+ Influx Activity Using Liposomes

	EC_{50} (sample/lipid) × 10^6		
compound	sterol-free liposomes	cholesterol-containing liposomes	ergosterol-containing liposomes
1 (AmB)	47	43	11
2 ($n = 4$)	61	86	50
3 ($n = 6$)	60	58	5.8
4 ($n = 8$)	180	110	27
5 ($n = 3,3$)	53	62	27

observed in this assay are described in recent publications.[17−22]

Figure 2 shows the concentration−effect relationships for **1**−**5** in ergosterol-containing liposomes. In this figure, the vertical axis denotes the reduction in the signal intensity at δ 1.2, which is equivalent to the increase in the ratio of permeabilized liposomes. Sigmoidal responses were observed for all of the compounds tested. From these curves, the molar ratio of AmB derivative/lipid at which 50% of liposomes were permeabilized was determined as EC_{50}. Table 1 lists the EC_{50} values of AmB and its derivatives in sterol-free, cholesterol-containing and ergosterol-containing liposomes. Although all of the compounds elicited membrane-permeabilizing actions, only derivative **3** showed a higher influx activity than that of AmB in ergosterol-containing liposomes. Interestingly, the effect of cholesterol is only marginal or rather inhibitory for all of the compounds tested. Recently, we have demonstrated that cholesterol prevents ion channel formation by membrane-bound AmB using similar preparations of liposomes.[19] These data further support the idea

(15) Herve, M.; Cybulska, B.; Gary-Bobo, C. M. *Eur. Biophys. J.* **1985**, *12*, 121−128.
(16) Herve, M.; Debouzy, J. C.; Borowski, E.; Cybulska, B.; Gary-Bobo, C. M. *Biochim. Biophys. Acta* **1989**, *980*, 261−272.
(17) Matsumori, N.; Yamaji, N.; Matsuoka, S.; Oishi, T.; Murata, M. *J. Am. Chem. Soc.* **2002**, *124*, 4180−4181.
(18) Yamaji, N.; Matsumori, N.; Matsuoka, S.; Oishi, T.; Murata, M. *Org. Lett.* **2002**, *4*, 2087−2089.
(19) Matsuoka, S.; Murata, M. *Biochim. Biophys. Acta* **2002**, *1564*, 429−434.
(20) Matsuoka, S.; Murata, M. *Biochim. Biophys. Acta* **2003**, *1617*, 109−115.
(21) Matsuoka, S.; Matsumori, N.; Murata, M. *Org. Biomol. Chem.* **2003**, *1*, 3882−3884.
(22) Matsumori, N.; Eiraku, N.; Matsuoka, S.; Oishi, T.; Murata, M.; Aoki, T.; Ide, T. *Chem. Biol.* **2004**, *11*, 673−679.

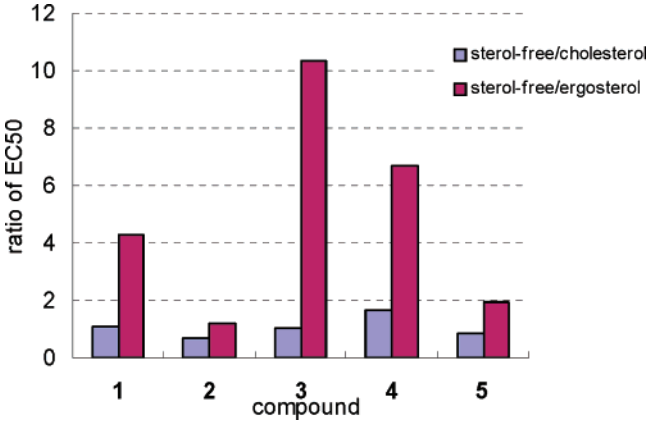

Figure 3. Sterol selectivity of compounds **1**−**5** expressed as a ratio of EC_{50} in sterol-free over that in sterol-containing liposomes (EC_{50} values are listed in Table 1). The higher index of ergosterol preference is obviously seen for **3** and **4**, while cholesterol has little effect on the activity of all of the compounds.

that cholesterol is not involved in formation of the channel complex.[19,23−26]

Figure 3 depicts ratios of the activity in sterol-containing membranes as compared to sterol-free membrane. Although the ergosterol preference in membrane permeability was somewhat observed in all of the derivatives prepared, the extent is markedly different among them. It is noteworthy that the ergosterol selectivity of compound **3** markedly exceeds that of AmB itself, whereas that of **2** was only marginal. The higher index of ergosterol selectivity for **3** as compared to **5** should be due to the fixation of the amino-sugar position in **3**. The drastic difference in sterol selectivity among bridged derivatives **2**−**4** is also likely to be attributable to changes in the orientations of the amino-sugar moiety induced by the different length of bridge chains.

NOE-Constrained Conformational Analysis. To address geometrical arrangements of the amino-sugars with respect to the macrolide portion in the bridged derivatives, we conducted conformational analyses using NMR data in DMSO solutions. If the structures of the derivatives are well rigidified by the intramolecular bridges, the solution structures should reproduce conformations occurring in the channel complex. Table 2 lists the assignments of ^{1}H NMR of AmB[27] and its derivatives in DMSO-d_6. The chemical shifts in the macrolide portions of the derivatives coincided well with those of AmB within 0.1 ppm except for the C16−C21 portion where the change in space arrangement of amino-sugar portions is likely to influence the chemical shifts. Spin-coupling patterns of the macrolide rings were also similar among the derivatives (data not shown). These observations indicate that no major change occurs in the macrolide conformation upon derivatization. Due to the possible inflexibility of the conjugated double bonds, the macrolide ring of AmB and derivatives was treated as a motion-restricted part, in which ±30° allowance from the crystal structure[28] was given to each C−C single bond upon calculations. Because our interests were focused on the location of amino-sugar moieties, this approximation in macrolide rings would not cause any significant errors.

Table 2. ^{1}H NMR Chemical Shifts for **1**−**5** in DMSO-d_6 at 25 °C (500 MHz)[a]

position	1	2	3	4	5
2	2.16	2.18	2.16	2.16	2.14
3	4.06	4.06	4.06	4.05	4.05
4	1.32, 1.38	n.d.	n.d.	n.d.	n.d.
5	3.51	3.54	3.52	3.51	3.49
6	1.26, 1.59	n.d.	n.d.	n.d.	n.d.
7	1.24, 1.56	n.d.	n.d.	n.d.	n.d.
8	3.09	3.11	3.07	3.10	3.10
9	3.48	3.37	3.45	3.44	3.45
10	1.31, 1.54	1.32, 1.49	n.d.	n.d.	n.d.
11	4.26	4.17	4.22	4.22	4.24
12	1.53	n.d.	n.d.	n.d.	n.d.
14	1.09, 1.86	1.03, 1.83	1.12, 1.85	1.06, 1.85	1.06, 1.86
15	3.99	3.99	4.00	4.01	4.02
16	1.93	2.05	1.90	1.85	1.86
17	4.18	4.17	4.32	4.01	4.23
18	1.54, 2.05	1.73, 1.83	1.50, 1.71	1.45, 1.88	1.42, 1.96
19	4.40	4.25	4.23	4.27	4.33
20	5.97	5.75	5.90	5.90	5.93
21	6.08	6.16	6.07	6.08	6.07
32	6.19	6.07	6.15	6.16	6.15
33	5.38	5.47	5.43	5.43	5.42
34	2.28	2.28	2.27	2.27	2.28
35	3.09	3.10	3.09	3.07	3.06
36	1.73	1.73	1.72	1.73	1.70
37	5.22	5.18	5.20	5.21	5.21
38	1.11	1.11	1.12	1.12	1.09
39	0.91	0.91	0.92	0.91	0.90
40	1.04	1.03	1.03	1.03	1.02
1′	4.61	4.36	4.36	4.25	4.23
2′	3.74	3.69	3.69	3.76	3.75
3′	2.81	2.40	2.39	2.24	2.28
4′	3.21	3.01	2.98	2.91	2.96
5′	3.25	3.18	3.12	3.07	3.04
6′	1.13	1.13	1.12	1.12	1.12
1″		2.71, 2.92	2.65, 2.76	2.56	2.44, 2.64
2″		1.77	1.46	n.d.	1.47
3″		1.77	1.21	n.d.	0.87
4″		2.69, 3.66	1.21	n.d.	2.92, 3.07
5″			1.46	n.d.	1.42
6″			2.74, 3.43	n.d.	0.84
7″				1.74	
8″				3.00	
amide		7.96	8.00	7.95	7.94

[a] n.d.: not determined due to signal overlapping.

Distance restraints for **2**−**5** were derived from 2D NOESY spectra in DMSO. The total number of inter-proton distance restraints derived from the NMR data was 22, 24, 14, and 20 for **2**, **3**, **4**, and **5**, respectively. On the basis of these conformational constraints, molecular modeling studies were performed using the Monte Carlo conformation search algorithm in MacroModel 8.5 package.[29] Figure 4 shows superposition of 20 lowest energy conformations around sugar portions of AmB derivatives **2**−**5**, in conjunction with the crystal structure of *N*-iodoacetylated AmB.[28] As expected, derivatives **2** and **3** have well converged conformers probably due to constraints of the short bridges. A slight but obvious difference in orientation of the amino-sugar portion with respect to the macrolide ring was seen between **2** and **3**, which is probably due to the difference in the length of bridges by two methylenes. Indeed, a short bridge of **2** appears to force the amino-sugar to locate closer to the C41

(23) Cotero, B. V.; Rebolledo-AntUnez, S.; Ortega-Blake, I. *Biochim. Biophys. Acta* **1998**, *1375*, 43−51.
(24) Dufourc, E. J.; Smith, I. C. P.; Jarrell, H. C. *Biochim. Biophys. Acta* **1984**, *776*, 317−329.
(25) Ruckwardt, T.; Scott, A.; Scott, J.; Mikulecky, P.; Hartsel, S. C. *Biochim. Biophys. Acta* **1998**, *1372*, 283−288.
(26) Cuntinho, A.; Prieto, M. *Biophys. J.* **1995**, *69*, 2541−2557.
(27) McNamara, C. M.; Box, S.; Crawforth, J. M.; Hickman, B. S.; Norwood, T. J.; Rawlings, B. J. *J. Chem. Soc., Perkin Trans. 1* **1998**, 83−88.
(28) Ganis, P.; Avitabile, G.; Mechlinski, W.; Schaffner, C. P. *J. Am. Chem. Soc.* **1971**, *93*, 4560−4564.
(29) Mohamadi, F.; Richards, N. G.; Guida, W. C.; Liskamp, R.; Lipton, M.; Canfield, C.; Chang, G.; Hendrickson, T.; Still, W. C. *J. Comput. Chem.* **1990**, *11*, 440−467.

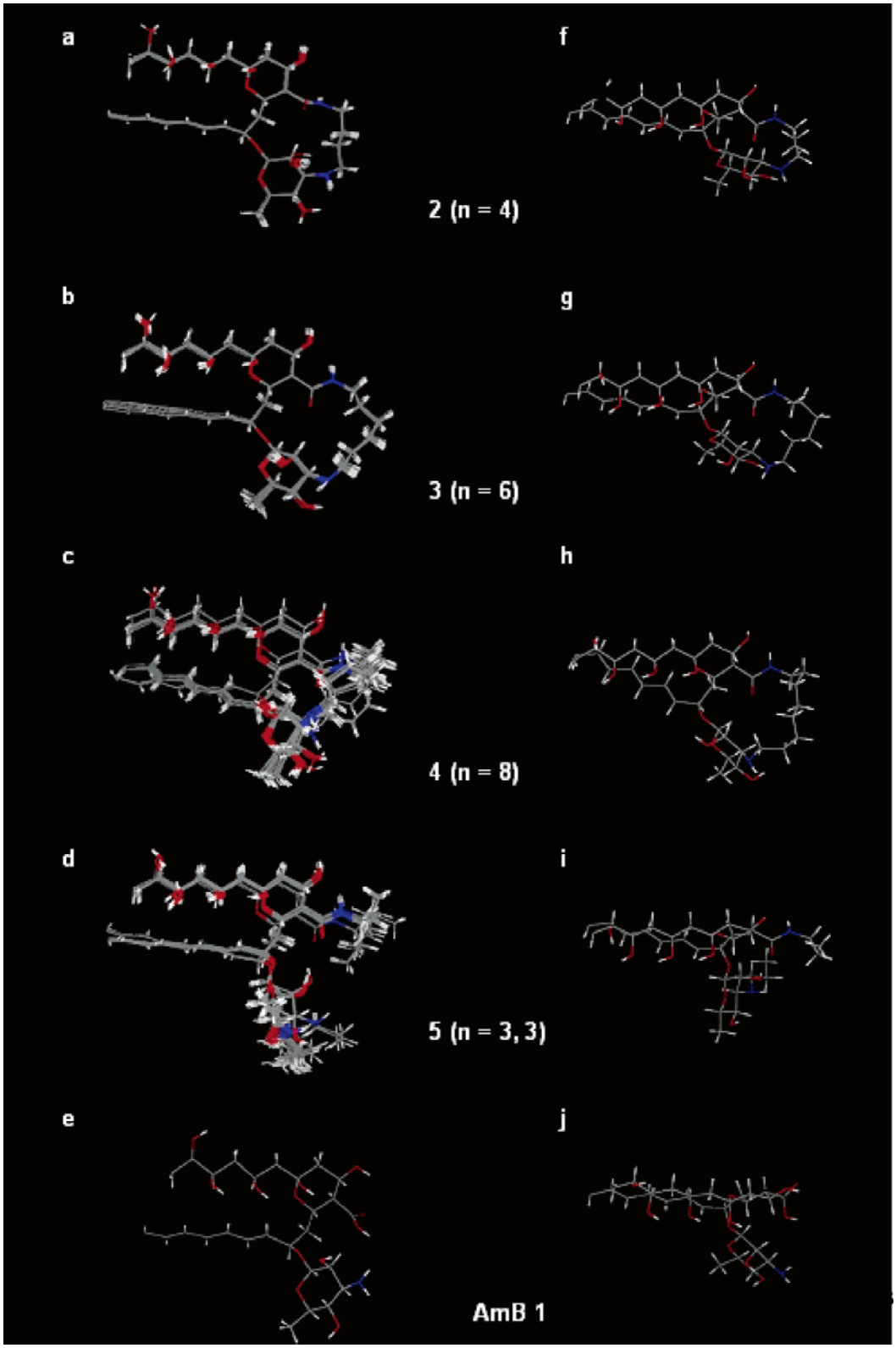

Figure 4. (a−d) Ensembles of 20 lowest energy conformations for **2**−**5**, generated by Monte Carlo algorithm restrained with distance constrains from 2D-NOESY in DMSO-d_6. Models are represented around polar head regions of molecules, and superposed for a minimum rmsd. (e) The structure of AmB from the crystal data of its *N*-iodoacetyl derivative is shown for comparison.[28] (f−i) Side views of the lowest energy conformers for (a−d), respectively. (j) Side view of (e).

carbonyl carbon, thus leading to the conformation that the plane of amino-sugar is nearly parallel to the macrolide plane. This alteration is evidenced by an NOE between H-2′ and amide proton, which is seen in **2** but not in **3**. In contrast, derivatives **4** and **5** yield fluctuated conformations for amino-sugar segments, probably due to a more flexible long bridge and an open chain structure, respectively.

Biological Activities. We then evaluated the membrane permeabilizing activity in biological systems. The derivatives **2**−**4** induced hemolysis against 1% human erythrocytes at the

Table 3. φ and ψ Angles (deg) of the Most Stable Conformers for Derivatives **2**−**4**[a]

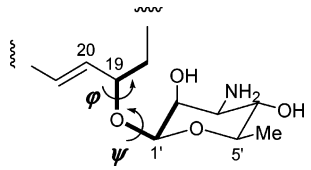

compound	φ	ψ
2 ($n = 4$)	−86.1	122.1
3 ($n = 6$)	−89.4	153.8
4 ($n = 8$)	−85.5	160.5

[a] The φ and ψ angles of the crystal structure of *N*-iodoacetylated AmB are −87.6° and 142.0°, respectively.[28]

concentration of 5.5, 2.2, and 2.2 μM, respectively, which is comparable to AmB (4.8 μM).[17] Because derivative **5** was decomposed in the conditions, we were unable to determine its hemolytic activity. The derivatives also revealed significant antifungal action against *Aspergillus nigar*, although less effective than AmB; the minimum amounts to show inhibitory zone on the culture of *A. nigar* are 10, 20, 50, and 10 μg per paper disk for derivatives **2**−**5**, respectively (AmB showed inhibitory zone at 5 μg).[17]

Discussion

The present results clearly demonstrate the importance of orientation of a mycosamine moiety relative to a macrolide ring in membrane permeabilizing activity of AmB. Derivative **2**, in which the amino-sugar adopts a parallel orientation with respect to the macrolide ring (Figure 4), shows less ergosterol selectivity, while derivative **3**, in which the plane of the sugar is somewhat twisted with respect to the macrolide, has the highest preference for ergosterol among the agents tested. Much less stimulatory effect by ergosterol for an open-bridged congener **5** rules out the possibility that *N*-alkyl substitution and/or amide formation at C41 augment ergosterol preference of AmB. The remarkable difference between **2** and **3** in sterol-dependent activity (Figure 3) discloses that a minute conformational alteration in the sugar part dramatically affects the sterol recognition by AmB; the conformational analysis reveals that the difference in ψ angles linkage between **2** and **3** is only 30° (Table 3). The possible conformations calculated in an aqueous environment converged well for **2** and **3**, which is indicative of the conformational rigidity. In addition, the macrocycles formed by AmB and bridges are reasonably deduced to expose to external water when bound to lipid bilayer, and macrocycles of these sizes are known to be able to adopt a well-defined 3-D structure even in water media if the macrocycles are sufficiently rigid.[30] It is, therefore, quite likely that the conformations of **2** and **3** are closely similar to those in Figure 4 when bound to lipid bilayer membrane.

Positions of the amino-sugar are defined by φ and ψ dihedral angles, where φ is C1′−O−C19−C18 and ψ is C2′−C1′−O41−C19. Baginski et al. have proposed that the arrangements between the amino-sugar moiety and the macrolide ring are largely dominated by two conformers: open (φ is ca. −150° and ψ is ca. 180°) and closed (φ is ca. −60° and ψ is ca. 180°) forms.[13h] In the open conformer, the amino and carboxyl groups are thought to form an intermolecular hydrogen bond with the complementary carboxyl and amino groups of the neighboring AmB molecules, thus facilitating AmB−AmB interactions. Conversely, the closed conformation is deduced to be responsible for formation of an intramolecular hydrogen bond between the carboxyl and the amino groups. The φ and ψ angles of the most stable conformers for derivatives **2**−**4** in our experiments (Table 3) are not coincident with Baginski's prediction. The present study shows that, as opposed to drastic conformational changes, rather minute conformational alteration can be attributable to the sterol preference of AmB.

The sterol dependence in membrane permeabilizing activity of AmB has been hitherto explained as a direct interaction with different binding affinity between the drug and sterols.[13j,16] The affinity is generally believed to be due to two types of interactions; one is a hydrogen bond between 3β-OH of sterol and the amino-sugar moiety of AmB either directly or mediated by water molecules,[13h−j,16] and the other is van der Waals force between AmB heptaene chromophore and hydrophobic steroid rings.[13b,j,31] The higher affinity of AmB toward ergosterol over cholesterol is often explained by the presence of an additional conjugated double bond, which allows the molecular proximity necessary to maximize the van der Waals interactions with AmB.[13j,31] Regarding the interaction of the mycosamine moiety and 3β-OH of sterols, Baginski et al. have proposed a model based on molecular dynamics simulations that 3′-NH_2 of AmB forms a hydrogen bond with 3β-OH of sterols,[13h] whereas Mazerski et al. postulated a hydrogen bonding between 2′-OH and 3β-OH of ergosterol.[13i] A close examination of the conformations calculated for **3** suggests that the interaction between the 3′-NH_2 of AmB and the 3β-OH of sterols is less probable because the amino group is faced away from the heptaene portion, with which hydrophobic sterol molecules are thought to interact. In contrast, the position of 2′-OH in **3** seems to allow for formation of the hydrogen bond with 3β-OH of the sterol molecule, thus supporting Mazerski's notion. Note that 2′-OH of compound **2** is more distant from the heptaene chromophore, and is thus seemingly unfavorable in interacting with sterol (as discussed later).

The biological activities of derivatives do not completely correlate with the results of ion-channel activity using artificial liposomes. It is difficult to completely account for the factors responsible for the discrepancy because there are significant differences between biological and model membranes: integral membrane proteins, lipid compositions, sterol contents, membrane charges, and the existence of cell wall in fungi. Particularly, in the antifungal test, the activity appears to decrease as the bridge chain lengthens. This is probably because polysaccharides of the cell wall form a strong diffusion barrier against hydrophobic molecules, which may cause difference in penetrability through the cell wall according to hydrophobicity of the bridged derivatives. More detailed investigations on biological activities of these derivatives are now in progress.

To better understand the mechanism of AmB's channel formation, the significance of AmB−phospholipid interaction as well as AmB−sterol should be appreciated.[32] Recent molecular dynamics simulations indicated the presence of electrostatic interaction between the amino-sugar of AmB and phos-

(30) Reid, R. C.; Kelso, M. J.; Scanlon, M. J.; Fairlie, D. P. *J. Am. Chem. Soc.* **2002**, *124*, 5673−5683.

(31) Charbonneau, C.; Fournier, I.; Dufresne, S.; Barwicz, J.; Tancrède, P. *Biophys. Chem.* **2001**, *91*, 125−133.

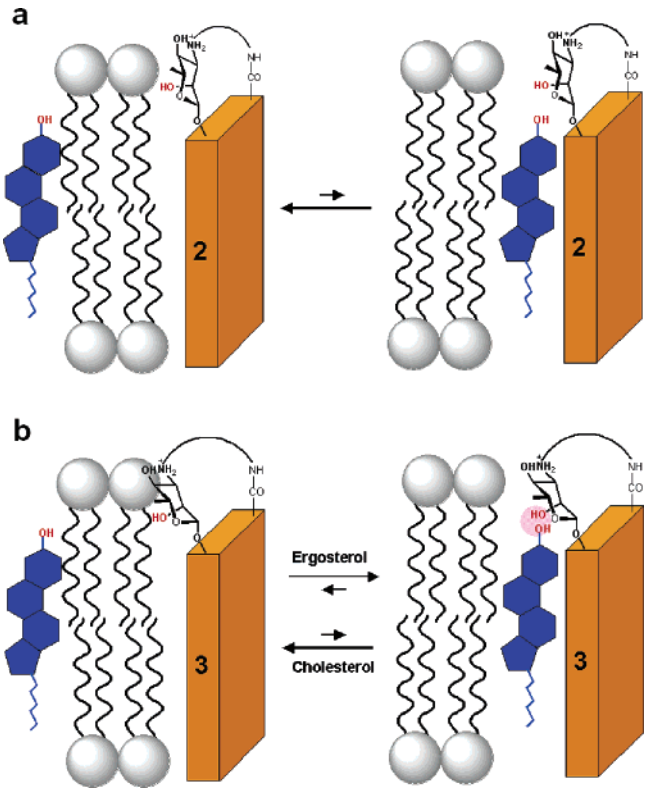

Figure 5. Schematic diagram for sterol selectivity in derivatives **2** and **3**. (a) For **2**, 3β-OH of sterol molecules are less interactive with 2′-OH of the amino-sugar moiety due to the distant location of the OH, and therefore sterol exerts little or no effect on the channel activity. (b) In derivative **3**, sterols can interact better due to the twisted orientation of the amino-sugar. An AmB−ergosterol complex with the greater hydrophobic interaction is more stable than AmB−cholesterol.

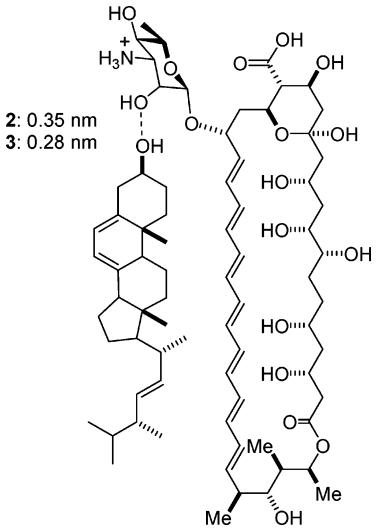

Figure 6. Possible interaction between AmB and ergosterol. Modeling experiments have revealed that 2′-OH of mycosamine of **3** is closer to 3-OH of ergosterol in the distance of 0.28 nm, which is the ideal length for hydrogen bonding, in comparison with that of **2**, 0.35 nm (see text for details).

phate of phospholipid,[13k] and very recently we have also succeeded in the direct observation of the close contacts between phosphate groups of phospholipid and AmB's polar part using a solid-state NMR technique.[33] Besides, it has been revealed that the length and/or saturation of phospholipid acyl chains also influence the channel activity of AmB, further indicating the importance of hydrophobic interactions between acyl-chain of phospholipid and AmB.[20,32d] Those results suggest the similarity in interaction modes between AmB−sterol and AmB−phospholipid. With this in mind, we hypothesize that both phospholipids and sterols can interact with the amino-sugar and heptaene regions of AmB as interaction sites, thus being rather competitive than cooperative upon complexation with AmB as implied in a previous report.[34] If this is the case, our data can be interpreted as in Figure 5; the amino-sugar orientation in **2** is unfavorable to form hydrogen bonding between 2′-OH of AmB and 3β-OH of sterols, and therefore sterol molecules cannot come close to **2**, thus making little or no effect on ion channel activity of **2**. In contrast, the amino-sugar moiety of derivative **3**, which is oriented so as to interact with sterol hydroxyl group, attracts a sterol molecule to the heptaene region close enough for the van der Waals contact. Ergosterol bearing the higher affinity for AmB heptaene can stay close to **3** and reinforce the channel structure. However, weakly interacting cholesterol molecules, even if they are drawn close to the heptaene region of **3** by the hydrogen bond between the amino-sugar and 3β-OH of cholesterol, might be easily replaced by phospholipid molecules (Figure 5), thus resulting in little or no effect on the channel activity.

The greater ergosterol selectivity of **4** than AmB is possibly ascribable to the conformation of the amino-sugar moiety, which is very close to that of **3** in the most stable conformer (Table 3). In contrast to its EC_{50} value in ergosterol-containing membrane, which is comparable with the other congeners (Table 1), **4** reveals weak activity for sterol-free membrane (Table 1). This may be due to its bulkier *N*-substituent, which possibly interferes with electrostatic interaction between **4** and phospholipid, and thus destabilizes the channel assemblage. However, **4** can accommodate ergosterol in the place of phospholipid because, upon interacting with the sterol, 2′-OH facing downward is not hindered by the *N*-substituent.

In the present study, we experimentally demonstrated that the relative positions of the mycosamine moiety have a strong influence on the sterol selectivity in channel activity of AmB by using conformation-restricted derivatives of AmB. Because the ion channel property of **3** is similar yet superior to that of AmB itself, the conformation of **3** is thought to reflect the active conformation of AmB in the channel complex to a considerable extent. The vertical position between AmB and ergosterol is reportedly restricted due to hydrophobic interaction.[13i] Our preliminary simulations for their bimolecular fitting based on van der Waals force also suggested the formation of stable complexes at a certain vertical position, although other intermolecular affects were not taken into account. As illustrated in Figure 6, when ergosterol is placed at this level, the distance between the 2′-**O**H of derivative **3** and 3-**O**H of ergosterol matches the stable hydrogen-bond length of 0.28 nm. On the

(32) (a) Ruckwardt, T.; Scott, A.; Scott, J.; Mikulecky, P.; Hartsel, S. C. *Biochim. Biophys. Acta* **1998**, *1372*, 283−288. (b) Cotero, B. V.; Rebolledo-Antunez, S.; Ortega-Blake, I. *Biochim. Biophys. Acta* **1998**, *1375*, 43−51. (c) Paquet, M. J.; Fournier, I.; Barwicz, J.; Tancrède, P.; Auger, M. *Chem. Phys. Lipids* **2002**, *119*, 1−11. (d) Miñones, J., Jr.; Dynarowicz-Latka, P.; Conde, O.; Miñones, J.; Iribarnegaray, E.; Casas, M. *Colloids Surf., B* **2003**, *29*, 205−215. (e) Fournier, I.; Barwicz, J.; Tancrede, P. *Biochim. Biophys. Acta* **1998**, *1373*, 76−86.
(33) Matsuoka, S.; Ikeuchi, H.; Matsumori, N.; Murata, M. *Biochemistry* **2005**, *44*, 704−710.
(34) Miñones, J., Jr.; Conde, O.; Miñones, J.; Rodriguez-Patino, J. M.; Seoane, R. *Langmuir* **2002**, *18*, 8601−8608.

contrary, the 2′-OH of **2** resides beyond the hydrogen-bonding limit with the same ergosterol position, thus supporting the notion in Figure 5. Although further experimental data should be necessary to elucidate the molecular interaction between AmB and ergosterol, the present results may provide clues to understand the structure basis for the drug's selective toxicity, which may lead to the design of new antibiotics with improved medicinal properties and less side effects.

Experimental Section

Materials and Methods. Amphotericin B (AmB), egg phosphatidylcholine, amino-alcohols, cholesterol, and ergosterol were from Nakarai Tesque. Deuterated solvents were purchased from Merck. All other chemicals were obtained from standard venders and used without further purification. NMR spectra were recorded on a JEOL GXS-500 spectrometer. ESI-MS spectra were measured on an LCQ-deca (Thermo Finnigan). HPLC was performed on a Shimadzu LC-10ADvp with SPD-M10Avp photodiode array detector. Thin-layer chromatography (TLC) was performed on a glass plate precoated with silica gel (E. Merck Kieselgel 60 F254). Column chromatography was performed with silica gel 60 (E. Merck, particle size 0.063−0.200 mm, 60−230 mesh).

***N*-(9-Fluorenylmethoxycarbonyl)-4-amino-1-butanol (6a).** To a stirred solution of 4-amino-1-buthanol (342 μL, 3.71 mmol) in MeOH (30 mL) were added 9-fluoromethyl succinimidyl carbonate (1000 mg, 2.96 mmol) and then pyridine (800 μL, 9.90 mmol). After being stirred at 23 °C for 23 h, the mixture was diluted with water (100 mL) and extracted with ethyl acetate. The organic layer was dried over $MgSO_4$ and concentrated in vacuo to give **6a** as white amorphous (920 mg, 100%). R_f 0.70 ($CHCl_3$:MeOH = 10:1). ^{1}H NMR (500 MHz, $CDCl_3$): δ 7.75 (d, 2H, J = 7.5 Hz), 7.57 (d, 2H, J = 7.5 Hz), 7.38 (t, 2H, J = 7.5 Hz), 7.30 (t, 2H, J = 7.5 Hz), 4.85 (brs, 1H), 4.39 (d, 2H, J = 6.5 Hz), 4.20 (t, 1H, J = 6.5 Hz), 3.66 (m, 2H), 3.23 (m, 2H).

***N*-(9-Fluorenylmethoxycarbonyl)-4-aminobutanal (7a).** A CH_2Cl_2 solution (5 mL) of DMSO (177 μL, 2.4 mmol) and a CH_2Cl_2 solution (10 mL) of **6a** (150 mg, 0.48 mmol) were added sequentially to a solution of oxalyl chloride (104 μL, 1.2 mmol) dissolved in CH_2Cl_2 (5 mL) at −78 °C. After being stirred for 30 min at −78 °C, the solution was treated with triethylamine (409 μL, 2.88 mmol) and stirred for 10 min at 0 °C. The resulting solution was diluted with water and extracted with diethyl ether. The organic layer was dried over $MgSO_4$, and concentrated in vacuo, yielding **7a** as white amorphous (130 mg, 94%). R_f 0.53 ($CHCl_3$:MeOH = 10:1). ^{1}H NMR (500 MHz, $CDCl_3$): δ 9.77 (s, 1H), 7.75 (d, 2H, J = 7.5 Hz), 7.57 (d, 2H, J = 7.5 Hz), 7.38 (t, 2H, J = 7.5 Hz), 7.30 (t, 2H, J = 7.5 Hz), 4.80 (br, 1H), 4.39 (d, 2H, J = 6.5 Hz), 4.20 (t, 1H, J = 6.5 Hz), 3.21 (m, 2H), 2.48 (m, 2H), 1.82 (m, 2H).

***N*-{*N*-(9-Fluorenylmethoxycarbonyl)-4-aminobututyl}-AmB (8a).** A solution of **7a** (13 mg, 43 μmol) and AmB (50 mg, 54 μmol) in DMF−MeOH (6:4, 10 mL) was stirred for 2 h, and then $NaBH_3CN$ (14 mg, 222 μmol) was added to the solution. After being stirred overnight, the solution was poured into diethyl ether (100 mL) to form a yellow precipitate, which was filtered over Celite and washed with diethyl ether. The precipitate on the Celite were extracted with $CHCl_3$−MeOH−H_2O 10:6:1 and purified by column chromatography on SiO_2 with the same solvent system to afford **7a** (23 mg, 44%) as a yellow solid. ESI-MS m/z 1217.7 $(M + H)^+$.

Derivative 2. To a solution of **7a** (23 mg, 19 μmol) in DMF−MeOH (1:1, 2 mL) was added piperidine (500 μL, 5 mmol). After the mixture was stirred for 30 min, diethyl ether was added to the solution to form a yellow precipitate. The precipitate was filtered over Celite and washed with diethyl ether. The product was extracted with $CHCl_3$−MeOH to give crude *N*-(4-aminobutyl)-AmB **8a** (16 mg), which was used for next reaction without further purification because of instability. To a solution of *N*-(4-aminobutyl)-AmB (16 mg) in DMF (2 mL) were added diisopropylethylamine (6 μL, 35 μmol), 1-hydroxybenzotriazole (3 mg, 20 μmol), and PyBOP (8.6 mg, 17 mmol) sequentially. After being stirred for 23 h, the mixture was poured into diethyl ether to form precipitate. The precipitate was filtered over Celite, washed with diethyl ether, and extracted with $CHCl_3$−MeOH. The extract was purified by HPLC to afford **2** (1.3 mg, 2.5%). HPLC conditions: column, COSMOSIL 5C_{18}-AR-II Φ 4.6 × 150 mm, flow rate, 0.5 mL/min, mobile phase, MeOH−5 mM ammonium acetate (pH 5.3) changing linearly from 70:30 to 100:0 for 30 min, retention time, 14.0 min. ESI-MS m/z 977.3 $(M + H)^+$. ^{1}H NMR (500 MHz, DMSO-d_6): see Table 2.

Derivative 3. *N*-(6-Aminohexyl)AmB **8b** was obtained by the procedure reported previously.[17] To a solution of **8b** (21 mg, 20 μmol) in DMF (2 mL) were added diisopropylethylamine (6.9 μL, 40 μmol), 1-hydroxybenzotriazole (3.7 mg, 24 μmol), and PyBOP (10.4 mg, 20 μmol) sequentially. After being stirred for 22 h, the mixture was poured into diethyl ether to form precipitate. The precipitate was filtered on Celite, washed with diethyl ether, extracted with $CHCl_3$−MeOH, and purified by HPLC to afford **3** (1.3 mg, 2.5%). HPLC conditions were the same as those for **2**, retention time: 16.5 min. ESI-MS m/z 977.3 $(M + H)^+$. ^{1}H NMR (500 MHz, DMSO-d_6): see Table 2.

***N*-(9-Fluorenylmethoxycarbonyl)-8-amino-1-octanol (6c).** 8-Amino-1-octanol, a known compound, was prepared by a modification of standard procedures. Briefly, 1,8-octanediol was treated with tosyl chloride, triethylamine, and (dimethylamino)pyridine in CH_2Cl_2 to give a mono-tosylated compound. The mono-tosylate was mixed with sodium azide in DMF to furnish 8-azido-1-octanol, which was then reduced by hydrogenation with Pd−C in MeOH to afford 8-amino-1-octanol. To a stirred solution of 8-amino-1-octanol (123 μL, 0.85 mmol) in MeOH (8 mL) were added 9-fluoromethyl succinimidyl carbonate (357 mg, 1.06 mmol) and then pyridine (185 μL, 2.29 mmol). After being stirred at 23 °C for 22 h, the mixture was diluted with water (100 mL) and extracted with ethyl acetate. The organic layer was dried over $MgSO_4$, and concentrated in vacuo, yielding **6c** as white amorphous (175 mg, 52%). R_f 0.26 ($CHCl_3$:MeOH = 10:1). ^{1}H NMR (500 MHz, $CDCl_3$): δ 7.75 (d, 2H, J = 7.5 Hz), 7.57 (d, 2H, J = 7.5 Hz), 7.38 (t, 2H, J = 7.5 Hz), 7.30 (t, 2H, J = 7.5 Hz), 4.71 (br, 1H), 4.38 (d, 2H, J = 7.0 Hz), 4.20 (t, 1H, J = 7.0 Hz), 3.62 (m, 2H), 3.17 (m, 2H).

***N*-(9-Fluorenylmethoxycarbonyl)-8-amino-1-octanal (7c).** To a DMSO solution (2.5 mL) of **6c** (85 mg, 0.23 mmol) were added sequentially triethylamine (600 μL, 3.5 mmol) and SO_3−Py (400 mg, 1.9 mmol). After being stirred for 30 min at 23 °C, the solution was diluted with water and extracted with diethyl ether. The organic layer was dried over $MgSO_4$, and concentrated in vacuo, yielding a crude mixture of **7c** (crude 73 mg), which was used without further purification.

***N*-{*N*-(9-Fluorenylmethoxycarbonyl)-8-aminooctyl}-AmB (8c).** A solution of **7c** (13 mg, 36 μmol) and AmB (50 mg, 54 μmol) in DMF−MeOH (4:3, 7 mL) was stirred for 2 h, and $NaBH_3CN$ (14 mg, 222 μmol) was added to the solution. After being stirred overnight, the solution was poured into diethyl ether (100 mL) to form a yellow precipitate, which was filtered over Celite and washed with diethyl ether. The precipitate was extracted with $CHCl_3$−MeOH−H_2O 10:6:1 and purified by SiO_2 column chromatography with the same solvent system to afford **8c** (28 mg, 41%) as a yellow solid. R_f 0.53 ($CHCl_3$:MeOH:H_2O = 10:6:1). ESI-MS m/z 1273.5 $(M + H)^+$.

Derivative 4. 8c (28 mg, 28 μmol) was dissolved in DMF−MeOH (1:1, 2 mL) and mixed with piperidine (500 μL, 5 mmol). After the mixture was stirred for 30 min, diethyl ether was added to the solution to form a yellow precipitate. The precipitate was isolated on Celite, washed with diethyl ether, and extracted with $CHCl_3$−MeOH to give crude *N*-(8-aminooctyl)-AmB **9c** (20 mg), which was used for next reaction without further purification. To a solution of **9c** (16 mg) in DMF (2 mL) were added diisopropylethylamine (6.6 μL, 38 mmol), 1-hydroxybenzotriazole (3.7 mg, 24 mmol), and PyBOP (10.4 mg, 20 mmol) sequentially. After being stirred for 21 h, the products were precipitated with diethyl ether (100 mL). The precipitate was extracted and purified with the same method as those for derivative **2**, HPLC

retention time: 20.4 min. ESI-MS *m*/*z* 1033.8 $(M + H)^+$. ^1H NMR (500 MHz, DMSO-d_6): see Table 2.

***N*-Propyl-AmB (10).** A solution of propionaldehyde (5 μL, 68 μmol) and AmB (50 mg, 54 μmol) in DMF−MeOH (4:3, 7 mL) was stirred for 2 h at room temperature, and then $NaBH_3CN$ (14 mg, 222 μmol) was added to the solution. The mixture was agitated overnight at room temperature, and the products were precipitated with diethyl ether (100 mL). The precipitate was extracted and purified in the same manner as that of **8a** to afford *N*-propyl-AmB (24 mg, 46%) as a yellow solid. R_f 0.54 ($CHCl_3$:MeOH:H_2O = 10:6:1). ESI-MS *m*/*z* 988.7 $(M + Na)^+$.

Derivative 5. To a solution of **10** (24 mg, 25 μmol) in DMF (2 mL) were added propylamine (3.1 μL, 38 μmol), diisopropylethylamine (9.2 μL, 52 μmol), 1-hydroxybenzotriazole (4.9 μg, 30 μmol), and PyBOP (13.6 mg, 25 μmol) sequentially. The mixture was stirred for 20 h at room temperature and precipitated with diethyl ether (100 mL). The precipitate was filtered on Celite, washed with ether, and purified by HPLC to give **5** as yellow powders. HPLC conditions were the same as those for **2**, retention time: 19.5 min. ESI-MS *m*/*z* 1007.4 $(M + H)^+$. ^1H NMR (500 MHz, DMSO-d_6): see Table 2.

NMR Measurements. The antibiotic solutions were prepared under dry argon in DMSO-d_6 at 3−5 mM concentration. All NMR spectra were recorded at 25 °C on a JEOL GSX500 spectrometer (^1H 500 MHz). Spectra were processed using Alice2 V.4.1 (JEOL DATUM) software. Homonuclear two-dimensional spectra COSY, TOCSY (HOHAHA), and NOESY were recorded with a 1.5 s recovery delay in the phase-sensitive mode using the States method as data matrixes of 512 (*F*1) × 1024 (*F*2) complex data points. Mixing times of 80 ms for TOCSY and 300 ms for NOESY spectra were used. The spectral width in both dimensions was 5000 Hz.

The data were apodized with shifted square sine-bell window functions in both *F*1 and *F*2 dimensions after zero-filling in the *F*2 dimension to obtain a final matrix of 512 (*F*1) × 2048 (*F*2) real data points. Chemical shifts were referenced to the solvent chemical shift (DMSO-d_5 (^1H), 2.49 ppm).

Experimental NMR Restraints. All of the interproton-distance restraints between non *J*-coupled protons are derived from the two-dimensional homonuclear NOESY experiments. Interproton restraints were classified into three categories. Upper bounds were fixed at 2.8, 3.4, and 4.0 Å for strong, medium, and weak correlations, respectively. A lower bound was fixed at 1.8 Å, which corresponds to the sum of the hydrogen van der Waals radii. Pseudo atom corrections of the upper bounds were applied for distance restraints involving the unresolved methylene and methyl protons (+1 Å). For stereospecifically assigned diastereotopic methylene protons, the interproton distances were applied to each proton according to the NOE peak intensities. When possible, H−C−C−H dihedral angles were restrained to dihedral domains according to the different $^3J_{HH}$ coupling constants measured using Karplus dihedral relations with ±30° allowance.

Structure Calculations. Models were calculated using the MacroModel software version 8.5[29] installed on RedHat Linux 8 OS. Initial atomic coordinates and structure files for each derivative were generated step by step from the crystal data of *N*-iodoacetyl AmB.[28] For each molecule, the macrolide rings were treated as semirigid group, in which ±30° allowance from the crystal structure[28] was given to each C−C single bond upon calculations. The sampling of the conformational space was performed following a Monte Carlo Multiple Minimum method.[35] The MMFF force field[36] implemented in the MacroModel was used. The non-bonded van der Waals' interactions were represented by a simple repulsive quadratic term. The experimental distance restraints were represented as a soft asymptotic potential, and electrostatic interactions were ignored. 5000 steps of MCMM were carried out for each molecule. Continuum solvation models for water using a Generalized Born/Surface Area (GB/SA)[37] were applied though the calculations.

Liposome Preparation. Large unilamellar vesicles (LUV) were prepared according to methods reported by Herve et al.[15] Briefly, egg phosphatidylcholine (52.0 μmol) or egg phosphatidylcholine-sterol (46.8 and 7.2 μmol) was dissolved in $CHCl_3$ (2 mL), and the mixture was evaporated to a thin film in a round-bottom flask. After being dried in vacuo for over 8 h, pH 7.5 buffer (0.726 mL) containing KH_2PO_4 (0.4 mM) and EDTA (1 mM) was added to the flask. The lipid mixture was suspended in the buffer by vortexing and sonication. The resultant suspension was frozen at −20 °C and thawed at 50 °C three times. The liposome solution thus obtained was passed repeatedly through a membrane filter (pore size, 0.2 μm, 19 times) with a Liposofast apparatus (AVESTIN), and then diluted with K_2SO_4 (0.4 M, 3.63 mL) to give 12 mM LUV solution.

K^+ Flux Assays Using ^{31}P NMR. For K^+ flux assays, the LUV suspension prepared above was adjusted to pH 7.5 with 10 M KOH. A 750 μL aliquot of the LUV suspension was transferred to a 1.5 mL Eppendorf tube and mixed with 2 μL of 10 mM carbonyl cyanide-*p*-trifluoromethoxyphenyl hydrazone (FCCP) ethanol solution and 2 μL of a DMSO solution of drugs. After incubation for 6 h at room temperature, a portion of 550 μL was transferred to a 5-mm NMR glass tube and mixed with 4.4 μL of 100 mM $MnCl_2$. ^{31}P NMR spectra were recorded at 23 °C on a JEOL GSX-500 spectrometer (^{31}P at 202.35 MHz) with ^1H-broad band decoupling. The assay was generally repeated more than three times for each sample with good reproducibility. The concentration−activity relationship shown in Figure 2 was depicted by varying sample−lipid molar ratios. The *y*-axis is a ratio of a decrease in peak area at δ 1.2. Sigmoid curves were fitted using Origin 6.1, from which EC_{50} values were determined.

Determination of Hemolytic Activity. Freshly collected human blood was centrifuged for 5 min at 1000*g*, and separated erythrocytes were washed twice by suspending in PBS buffer (pH 7.4). Packed erythrocytes were then resuspended with PBS to 100-fold volume of the original blood. Gradually, diluted drug solutions (DMSO solution, 2 μL) were added to the erythrocyte suspensions (198 μL), and the suspensions were incubated with gently shaking at 37 °C. After 18 h, the suspensions were spun and the absorbance of the supernatant was determined at 490 nm by micro-plate reader (Molecular Devices). For a positive control, water was used instead of PBS buffer. As a negative control, 2 μL of DMSO was added instead of sample solution. From dose−response curves, the dosage that led to 50% hemolysis (EC_{50}) was determined.

Antifungal Assay. *Aspergillus nigar* was cultured in a GP liquid medium (2% glucose, 0.2% yeast extract, 0.5% polypeptone, 0.05% $MgSO_4$, and 0.1% KH_2PO_4) at 25 °C for 2 days. An aliquot of the broth was then spread onto a GP agar plate. The drugs dissolved in DMSO were spotted on paper disks of 8 mm in diameter. As a control, a disk containing only DMSO was also prepared. These paper disks were then placed on an agar plate containing *A. nigar* mycelia. After cultivating at 25 °C for 2 days, the diameter of the inhibitory zone on each paper disk was measured.

Acknowledgment. We are grateful to Ms. Rie Masuda, Prof. Tohru Oishi, and Dr. Shigeru Matsuoka in our laboratory for invaluable discussions. This work was supported by Grant-In-Aids for Scientific Research on Priority Area (A) (No. 12045243) and for Young Scientists (B) from the Ministry of Education, Sciences, Sports, Culture, and Technology, Japan, and by a grant from CREST, Japan Science and Technology Corp.

Supporting Information Available: NMR spectra and NOE correlations for **2**−**4**. This material is available free of charge via the Internet at http://pubs.acs.org.

JA051597R

(35) Kolossvary, I.; Guida, W. C. *J. Comput. Chem.* **1999**, *20*, 1671−1684.
(36) Halgren, T. A. *J. Comput. Chem.* **1999**, *20*, 730−748.
(37) Qiu, D.; Shenkin, P. S.; Hollinger, F. P.; Still, W. C. *J. Phys. Chem. A* **1997**, *101*, 3005−3014.